High-filling-fraction inverted ZnS opals fabricated by atomic layer deposition

J. S. King,[a] C. W. Neff, and C. J. Summers[b]
School of Materials Science and Engineering, Georgia Institute of Technology, Atlanta, Georgia 30332-0245

W. Park
Department of Electrical and Computer Engineering, University of Colorado, Boulder, Colorado 80309-0425

S. Blomquist, E. Forsythe, and D. Morton
Army Research Laboratory, Adelphi, Maryland 20783-1145

(Received 12 May 2003; accepted 12 July 2003)

The infiltration of three-dimensional opal structures has been investigated by atomic layer deposition. Demonstrations using ZnS:Mn show that filling fractions $>95\%$ can be achieved and that the infiltrated material is of high-quality crystalline material as assessed by photoluminescence measurements. These results demonstrate a flexible and practical pathway to attaining high-performance photonic crystal structures and optical microcavities. © *2003 American Institute of Physics.* [DOI: 10.1063/1.1609240]

The work of John[1] and Yablonovitch[2] in the late 1980's has resulted in an extensive interest in the fabrication of photonic crystals. Numerous methods have been employed to make such structures[3–6] and a complete photonic band gap has been demonstrated in millimeter[3] and infrared[4,6] wavelengths. The requirements for a complete photonic band gap include: high refractive index contrast (>2.8), long-range three-dimensional periodicity, and a high filling fraction. Many groups have shown that the infiltration of opals is a suitable route for obtaining the desired periodic structure.[6–10] Most of these studies have involved variations of chemical bath deposition and report low filling fractions. The exceptions have been ZnS,[11] which has been incorporated with approximately 50% filling of the interstitial volume and CdS,[12] with filling fractions as high as 96%. However, this technique tends to produce many nanocrystallites such that the luminescent properties are very poor and usually the resulting structures exhibit low filling fractions due to high porosity. Also, chemical vapor deposition has been used for infiltration exhibiting filling fractions ranging from 1% to 100%, with the highest numbers being for silicon which is not a luminescent material.[6–9]

In this letter, we report a method of fabricating inverse opal films that utilizes atomic layer deposition (ALD) for the infiltration step. ALD is a growth technique that utilizes the sequential application of reactants coupled with substrate temperature optimization to achieve monolayer-by-monolayer growth.[13] As a result, growth is surface controlled instead of source controlled, enabling highly controllable deposition of conformal films on substrates with complex geometries,[14] such as opals.

For this study colloidal silica solutions containing monodispersed spheres, 145–500 nm in diameter, were formed by the Stober method.[15] Self-assembled face centered cubic silica opal templates were then formed on silica or silicon substrates by the sedimentation of monodispersed colloidal silica in confinement cells as pioneered by Park *et al.*,[16] and then dried and sintered (700–800 °C for 2 h) to enhance structural stability, and to provide interconnectivity between the spheres. The interstitial volume of the opal was next filled with ZnS:Mn using conventional ALD precursors. Etching the infiltrated films in a 2% HF solution resulted in the removal of the silica spheres, and the formation of structurally stable inverse opals. The films were characterized using specular reflectivity, scanning electron microscopy (SEM), and photoluminescence (PL) both after infiltration and after etching. The resulting opal films were polycrystalline, 10-μm-thick, 2 cm$\times$2 cm squares, with the (111) planes oriented parallel to the substrate as is typically seen in confinement cell grown opal.[17] Grain sizes were typically on the order of $\sim 100\ \mu$m wide. After sintering, the specular reflectivity was measured to confirm the lattice constants of the resulting opals by analysis of the (111) Bragg peak position. The calculated plane spacing agreed well with measurements of colloidal silica sphere sizes obtained using a transmission electron microscope.

ZnS was used as a prototype material because when doped it is highly luminescent with a wide range of emission wavelengths and it is also a well-studied material for ALD. However, its refractive index is too low (~ 2.5) for the formation of a full photonic band gap but high enough to produce a pseudogap. ZnS was grown using $ZnCl_2$ and H_2S reactants at 500 °C using a flow style reactor (Microchemistry, Ltd). The substrate was first exposed to a 660 ms $ZnCl_2$ gas pulse, which resulted in the chemiadsorption of a monolayer of molecules on the surface.[18] The substrate was next purged with N_2 for 550 ms to remove any excess $ZnCl_2$. Conversion to ZnS was accomplished by application of a 660 ms H_2S pulse to the substrate. An additional 550 ms N_2 pulse to remove excess H_2S and the HCl byproduct completed the cycle. This sequence resulted in a partial monolayer of ZnS

[a]Electronic mail: jeffrey.king@mse.gatech.edu
[b]Electronic mail: chris.summers@mse.gatech.edu

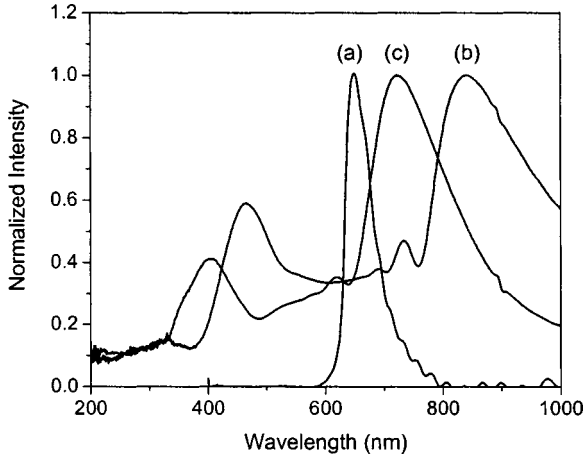

FIG. 1. Reflectance spectra measured for a 300 nm opal. (a) Bare opal exhibiting (111) Bragg peak at 652 nm (normal incidence), (b) as-infiltrated opal exhibiting (111) Bragg peak, at 843 nm. (15 deg. incidence), (c) inverse opal exhibiting (111) Bragg peak at 726 nm (15 deg. incidence).

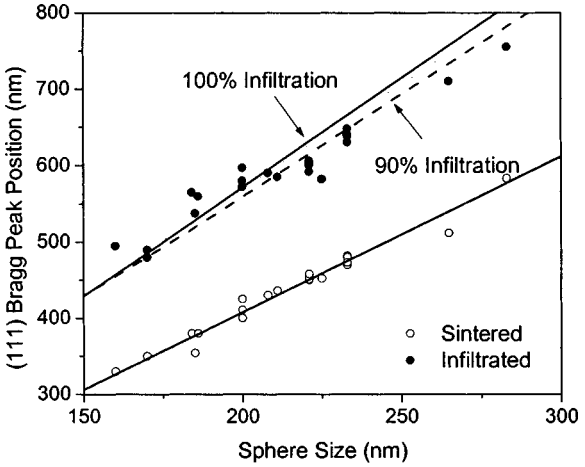

FIG. 2. Bragg Peak position as a function of sphere size for sintered and ZnS infiltrated SiO2 opals.

(0.78 Å per cycle), which was repeated to precisely grow a film layer by layer. The film thickness was varied based on the opal sizes; 47 nm films were grown for opals 220 nm and below, and 70 nm films were grown for 300 nm opals. For this study, an excess of ZnS was always grown on the opal, since the voids in the opal require less the thickness of the layer to fill. To fabricate optically active photonic crystals, Mn^{2+} was added as a luminescent center by incorporating $MnCl_2$ with $ZnCl_2$ during every 100th pulse cycle.

When viewed with the naked eye the resulting films exhibit uniform angular dependent colors, indicating that the infiltration was homogeneous throughout the opaline film. The (111) Bragg peak position was determined from specular reflectance measurements taken before and after infiltration, and after etching, and was used to calculate the filling fraction of the interstitial volume. The Bragg peak corresponds to the first stop band at the L point in the photonic band structure and using bulk values for the silica and ZnS refractive indices enables calculation of the filling fraction. Figure 1 shows typical reflectance spectra for 300 nm sintered, infiltrated, and etched opals. As expected, after infiltration the peak shifts to longer wavelengths due to an increase in the average refractive index. Also the gap-to-midgap ratio increases, and is in agreement with the photonic band structures that were calculated using a plane-wave expansion software package.[19] After etching, the inverse opal exhibited a shift of the reflectance peak to a longer wavelength, corresponding to the consequent decrease in the average refractive index. The gap-to-midgap ratio was also observed to increase due to the increase in refractive index contrast resulting from the removal of the silica spheres. This behavior was confirmed by the calculated band structures, which predicts a shift of the photonic band gap to higher frequencies for the inverse opal structure. The reflectivity peaks were found to correspond to the mid-gap frequency of the pseudogap in the $\Gamma - L$ direction of their respective band structure diagrams. Also these calculations showed that the width of the pseudogap increases in the inverted opal structure, reinforcing the widening of the reflectivity peak seen in the spectrum.

ALD infiltrations were performed on opals with sphere sizes ranging from 145 to 460 nm and specular reflectivity was measured for each sample. The dependence of the Bragg peak position before and after sintering as a function of sphere size is shown in Fig. 2, with the data fitted to give the average trend lines shown. From the trend line for the infiltrated opal, the average fill fraction was $>90\%$ of the available pore volume. For small lattice constant opals (<220 nm) the data are consistently above the 100% infiltrated. The reason for this is unknown, but could be attributed to a breakdown in the effective dielectric medium theory. To demonstrate the flexibility of this technique we have also performed partial infiltrations, of 27% and 57% by depositing ZnS coatings of ~ 2 and ~ 5 nm, thick, respectively.

To ensure that ALD-deposited ZnS exhibits the bulk refractive index, a thick film was grown and its refractive index measured using a Filmetrics F20 thin film analysis tool. These measurements gave values ranging from 2.31 to 2.53 for wavelengths between 800 and 400 nm, respectively, in good agreement with published data.[20] Therefore, the observed peak shifts can only be accounted for by the full infiltration of the opal by high-quality ZnS. Thus, it is concluded that ALD-deposited ZnS exhibits the bulk material's ordinary refractive index, which is often difficult to achieve using methods that utilize solution precipitation.[21]

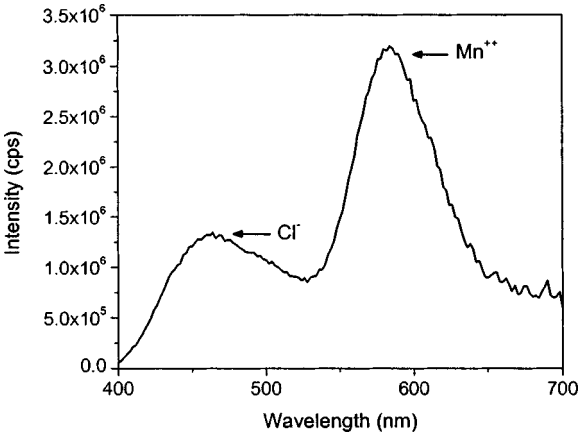

FIG. 3. Photoluminescence of 225 nm ZnS:Mn infiltrated opal, 330 nm excitation.

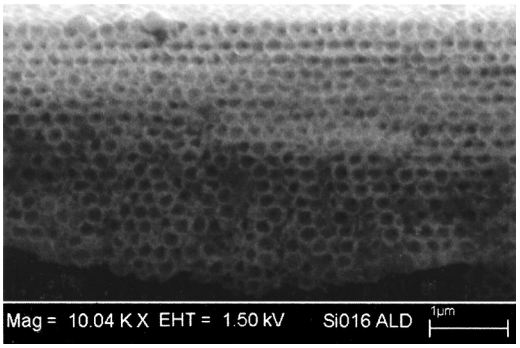

FIG. 4. SEM of a cleaved 220 nm ZnS:Mn inverse opal.

Photoluminescence measurements were used to assess the quality of the infiltrated material. Figure 3 shows a typical PL spectra of the infiltrated films excited by 330 nm radiation. The luminescence intensity was measured to be as strong or stronger than that observed from codeposited ZnS:Mn thin films. In Fig. 3 the broadband PL peak at 585 nm is due to Mn^{2+} emission, and the peak at 460 nm is due to doping by Cl^{-}, which arises as a result of the $ZnCl_2$ precursor. Inverted structures were obtained by immersing the infiltrated opals in a 2% HF solution for 2 h. Since the films were lightly sintered, flow channels are available throughout the structure for the HF to etch out all of the spheres. After rinsing and drying, successful inversion was evident by the noticeable color change of the reflected light from the surface of the opal. This color change was quantified by performing specular reflectance measurements. The resulting film was cleaved and examined in a SEM. Figure 4 shows a cross section of the inverted opal structure. In addition, the inverted opals were found to be highly luminescent from PL measurements.

In summary, we have demonstrated that ALD has high potential as a flexible infiltration method for the fabrication of inverse opal structures. The technique has been shown to produce infiltrations with filling fractions as high as 100% of the available interstitial volume. The material deposited exhibits high crystalline quality, as is shown by the attainment of the full refractive index of the ZnS infiltrate, and the strong photoluminescence observed. Since ALD can be used for the deposition all classes of materials, it holds great potential for the growth of highly luminescent materials, high refractive index materials and also multilayered materials.

The authors acknowledge discussions with Dr. Shawn-Yu Lin and thank support from the Army Research Office under Contract No. DAAD19-01-1-0603 and Sandia National Laboratories, Contract No. 18499.

[1] E. Yablonovitch, Phys. Rev. Lett. **58**, 2059 (1987).
[2] S. John, Phys. Rev. Lett. **58**, 2486 (1987).
[3] E. Yablonovitch, Phys. Rev. Lett. **67**, 2295 (1991).
[4] E. Özbay, E. Michel, G. Tuttle, R. Biswas, M. Sigalas, and K.-M. Ho, Appl. Phys. Lett. **64**, 2059 (1994).
[5] S. Y. Lin, J. G. Fleming, D. L. Hetherington, B. K. Smith, R. Biswas, K. M. Ho, M. M. Sigalas, W. Zubrzycki, S. R. Kurtz, and J. Bur, Nature (London) **394**, 251 (1998).
[6] A. Blanco, E. Chomski, S. Grabtchak, M. Ibisate, S. John, S. W. Leonard, C. Lopez, F. Meseguer, H. Miguez, J. P. Mondia, G. A. Ozin, O. Toader, and H. M. Driel, Nature (London) **405**, 437 (2000).
[7] Y. A. Vlasov, X-Z Bo, J. C. Sturm, and D. J. Norris, Nature (London) **414**, 289 (2001).
[8] H. M. Yates, W. R. Flavell, M. E. Pemble, N. P. Johnson, S. G. Romanov, and C. M. Sotomayor Torres, J. Cryst. Growth **170**, 611 (1997).
[9] S. G. Romanov, R. M. De La Rue, H. M. Yates, and M. E. Pemble, J. Phys.: Condens. Matter **12**, 339 (2000).
[10] W. Park, J. S. King, C. W. Neff, C. Liddell, and C. J. Summers, Phys. Status Solidi B **229**, 949 (2002).
[11] S. G. Romanov, A. V. Fokin, and R. M. De La Rue, Appl. Phys. Lett. **74**, 1821 (1999).
[12] A. Blanco, H. Míguez, F. Meseguer, C. López, F. López-Tejeira, and J. Sánchez-Dehesa, Appl. Phys. Lett. **78**, 3181 (2001).
[13] T. Suntola and M. Simpson, *Atomic Layer Epitaxy*, 1st ed. (Chapman and Hall, New York, 1990), Chap. 1, p. 1.
[14] O. Sneh, R. Clark-Phelps, A. Londergan, J. Winkler, and T. Seidel, Thin Solid Films **402**, 248 (2002).
[15] W. Stober, A. Fink, and E. Bohn, J. Colloid Interface Sci. **26**, 62 (1968).
[16] S. H. Park, D. Qin, and Y. Xia, Adv. Mater. (Weinheim, Ger.) **10**, 1028 (1998).
[17] Y. Xia, B. Gates, and S. H. Park, J. Lightwave Technol. **17**, 1956 (1999).
[18] M. A. Herman, Appl. Surf. Sci. **112**, 1 (1997).
[19] S. G. Johnson and J. D. Joannopoulos, Opt. Express **8**, 173 (2001).
[20] E. D. Palik, *Handbook of Optical Constants of Solids* (Academic, San Diego, CA, 1998) Vol. 1, Chap. 11, p. 597.
[21] G. Subramania, K. Constant, R. Biswas, M. M. Sigalas, and K.-M. Ho, J. Lightwave Technol. **17**, 1970 (1999).